Magnetotail Configuration under Northward IMF Conditions

Wenhui Li[1], leyuan wu[1], Yasong S Ge[2], and Lianzhong Lü[3]

[1]Zhejiang University of Technology
[2]Institute of Geology and Geophysics
[3]Guangxi University

November 22, 2022

Abstract

Due to the sparsity of space probes, it is still not clear on how the magnetic structure of the magnetotail looks like and how it evolves when the Interplanetary Magnetic Field (IMF) directs northward. This simulation study uses two different global magnetosphere MHD models to simulate two northward IMF events and study the evolution of the magnetotail. Both models show that the magnetotail may form a structure that is composed of a dawnside tail lobe and a duskside tail lobe instead of a northern tail lobe and a southern tail lobe under southward IMF conditions. In this magnetic configuration, a tail lobe extends a domain from northern (southern) cusp to southern (northern) IMF. The bigger the magnitude of IMF clock angle, the longer and wider the magnetotail. Such magnetic configuration suggests that magnetotail reconnection is possible to occur when the dawnside tail lobe contacts with the duskside tail lobe and thus a substorm is also possible to occur under northward IMF conditions with significant *By*.

Magnetotail Configuration under Northward IMF Conditions

Wenhui Li[1], Leyuan Wu[1], Yasong Ge[2,3,4], and Lian-Zhong Lü[5]

[1]College of Science, Zhejiang University of Technology, Hangzhou, China.

[2]Key Laboratory of Earth and Planetary Physics, Institute of Geology and Geophysics, Chinese Academy of Sciences, Beijing, China.

[3]University of Chinese Academy of Sciences, Beijing, China.

[4]Institutions of Earth Science, Chinese Academy of Sciences, Beijing, China.

[5]Astrophysics and Space Science Center, Guangxi University, Nanning, China.

Corresponding author: Wenhui Li (WenhuiLi88@yahoo.com)

Key Points:

- A dawnside tail lobe and a duskside tail lobe may form in the magnetotail under northward IMF conditions with significant *By*.
- The bigger the magnitude of IMF clock angle, the longer and wider the magnetotail.
- Magnetotail reconnection may occur when the dawnside tail lobe contacts with the duskside tail lobe, and is possible to cause substorm.

Abstract

Due to the sparsity of space probes, it is still not clear on how the magnetic structure of the magnetotail looks like and how it evolves when the Interplanetary Magnetic Field (IMF) directs northward. This simulation study uses two different global magnetosphere MHD models to simulate two northward IMF events and study the evolution of the magnetotail. Both models show that the magnetotail may form a structure that is composed of a dawnside tail lobe and a duskside tail lobe instead of a northern tail lobe and a southern tail lobe under southward IMF conditions. In this magnetic configuration, a tail lobe extends a domain from northern (southern) cusp to southern (northern) IMF. The bigger the magnitude of IMF clock angle, the longer and wider the magnetotail. Such magnetic configuration suggests that magnetotail reconnection is possible to occur when the dawnside tail lobe contacts with the duskside tail lobe and thus a substorm is also possible to occur under northward IMF conditions with significant *By*.

Plain Language Summary

The Earth's magnetosphere is a vast space with certain magnetic structure and plasma material and is directly affected by solar wind and its embedded magnetic field named Interplanetary Magnetic Field (IMF). Due to the sparsity of space probes, it is still not clear on how the magnetic structure of the magnetosphere looks like and how it evolves, especially when the IMF arriving the magnetosphere directs northward with a significant dawn-dusk component *By*. This simulation study uses two different global magnetosphere models to simulate the magnetosphere for two periods with northward IMF and show that the magnetotail (tail of magnetosphere) may form a structure that is composed of a dawnside tail lobe and a duskside tail lobe instead of a northern tail lobe and a southern tail lobe under southward IMF conditions. In this magnetic configuration, a tail lobe extends a domain from northern (southern) cusp to southern (northern) IMF. The bigger the IMF *By*, the longer and wider the magnetotail. Such magnetic configuration suggests that magnetotail reconnection is possible to occur when the dawnside tail lobe contacts with the duskside tail lobe and thus a substorm is also possible to occur under northward IMF conditions with significant *By*.

1 Introduction

The fundamental physical process in the Earth's space is the magnetic reconnection that merges two domains of plasma with antiparallel magnetic field relative to each other at their contacting site (Dungey, 1961, 1963). The Earth's magnetosphere is thus mainly affected by the direction of the interplanetary magnetic field (IMF) embedded with solar wind plasma, as the geomagnetic dipole direction is always mainly northward.

When IMF is southward, it is well known that there are two reconnection processes that mainly form the magnetosphere's magnetic configuration. First, IMF field lines interconnect with geomagnetic field lines at dayside magnetopause when solar wind plasma hits on the Earth's magnetosphere, creating two sets of open field lines that consequently are convected toward nightside of the Earth due to the frozen-in condition of collisionless plasma and form two plasma domains which are the northern magnetic tail lobe and the southern magnetic tail lobe. Secondly, when these two plasma domains contact with each other, the northern open field lines reconnect with the southern open field lines and create new IMF field lines and new closed field lines.

When IMF is northward, there are two magnetic reconnection sites at the nightside of the cusps of the Earth's dipole field, as indicated by the northern point M1 and the southern point M2 in Figure 1. At these two sites, a draped IMF field line is antiparallel with an open field line or a closed field line. Such reconnection is called cusp reconnection, lobe reconnection, or high latitude reconnection (Cowley 1981; Dungey, 1963; Fuselier et al., 2000; Lavraud et al., 2005b, 2006; & Li et al., 2008; Onsager et al., 2001; Phan et al., 2003; Russell, 1972). However, the scenario of cusp reconnection has more variations than the dayside magnetopause reconnection, because there are two reconnection sites and two types of geomagnetic field lines that a draped IMF field line may encounter.

In theory, there are two main scenarios as following. A draped IMF field line may only merge with the geomagnetic field at one of the two merging sites, resulting in a new open field line draping the dayside magnetopause and a new open field line or a new IMF field line in the tail depending on what type of geomagnetic field line merging at M1 or M2. Or a draped IMF field line merges with the geomagnetic field at both merging sites, resulting in a new closed field line draping the dayside magnetopause and new open field line(s) and/or new IMF field line(s). The newly created field lines then are all convected tailward. However, it is not clear how such open field lines are distributed in the tail.

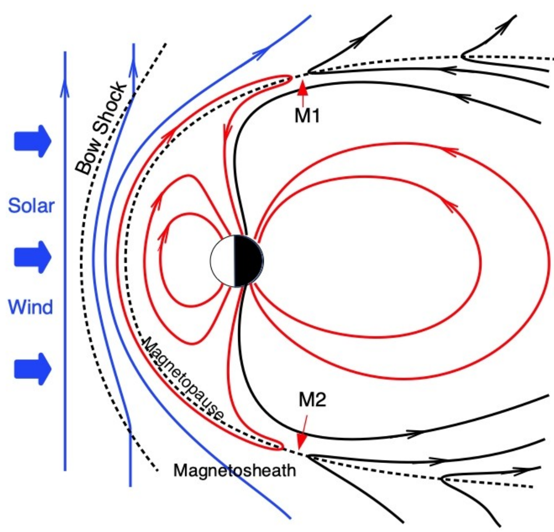

Figure 1. Magnetospheric field configuration of magnetosphere for pure northward IMF . Blue and red lines represent IMF field lines and closed field lines, respectively; But a solid black line may be IMF, open, or closed field line. M1 or M2 indicates a magnetic reconnection site. This is a view from the duskside of the magnetosphere.

In this study, we use two different global magnetosphere MHD models to simulate two events whose IMF is northward with a significant *By*, and study the configuration and evolution of the magnetotail. We also discuss the possible magnetotail reconnection and substorm that may occur during northward IMF conditions.

2 Method

We use global magnetosphere models BATS-R-US and OpenGGCM hosted on NASA Community Coordinated Modeling Center (CCMC) to simulate two northward IMF events . We also use the plotting services provided by CCMC to analysis the simulation results. Therefore, all our simulation output datasets are stored in CCMC and can be openly analyzed through CCMC portal (http://ccmc.gsfc.nasa.gov).

On an adaptive mesh refinement grid, BATS-R-US solves the global MHD equations for the magnetosphere using numerical methods related to Roe's Approximate Riemann Solver (Powell et al., 1999; Tóth et al, 2012). Its built-in ionospheric potential solver provides electric potentials and conductances in the ionosphere from magnetospheric field-aligned currents. On a stretched Cartesian grid, OpenGGCM solves the global magnetosphere MHD equations using second order explicit time integration with conservative and flux-limited spatial finite differences (Raeder, 2003). It is coupled with Coupled Thermosphere Ionosphere Model (CTIM) (Fuller-Rowell et al., 1996). More detail information about these models can be accessed through CCMC portal.

We use BATS-R-US 20140611version and OpenGGCM 4.0 version without coupling ring current or radiation belt model. CTIM is used in OpenGGCM simulations. The run numbers on CCMC are Wenhui_Li_062216_1, Wenhui_Li_062216_2, Wenhui_Li_081516_1, and Wenhui_Li_081516_2. Solar wind and IMF data from NASA OMNI is used to drive the models. High resolution grid of 9.0 million cells is used for both models. The two simulated events are from 2000:09:17 20:00:00 UT to 2000:09:18 08:00:00 UT and from 2000:08:12 20:00:00 UT to 2000:08:13 02:00:00 UT. During the first event, the IMF is northward from 00:00 UT to 08:00 UT as shown in Figure 2. For the second event, the IMF is northward from 18:00 UT to 02:00 UT the next day. Both events have significant IMF *By* component. In this presentation, we will focus on results from the simulation of the first event. During this event, the IMF is first

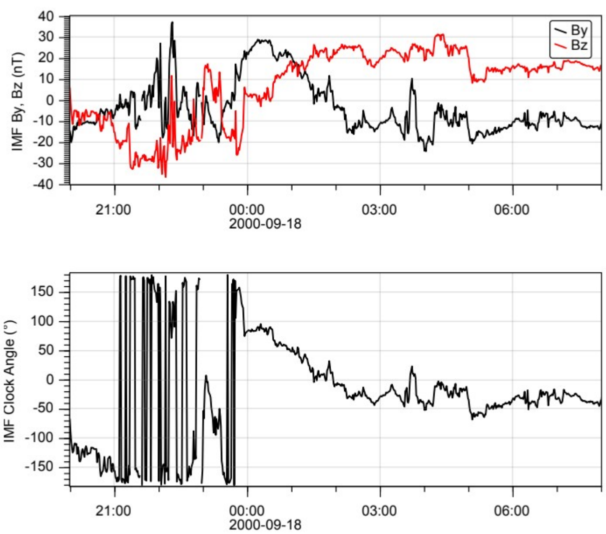

Figure 2. IMF conditions for event1 near dayside magnetopause. The time range is from 2000:09:17 20:00 UT to 2000:09:18 08:00 UT. The panels from top to bottom are IMF *By* and *Bz* components in GSM coordinates, and IMF clock angle (atan(*By*/*Bz*)).

southward and then changes to northward. The solar wind speed is on 700 km/s level during this event.

In this study, we inspect the magnetosphere by showing the distribution of four types of magnetic field lines. These four types of magnetic field line are closed geomagnetic field line connecting both cusps, IMF field line, open geomagnetic field line connecting northern cusp with southern IMF, and open geomagnetic field line connecting southern cusp with northern IMF. For a point on the equatorial plane, we trace the magnetic field line passing through it, and color it according to the topology of this field line: red for closed field line, blue for IMF field line, green for open field line rooted in southern cusp, and yellow for open field line rooted in northern cusp.

3 Simulation Results

3.1 Magnetotail under southward or northward IMF conditions

Figure 3 shows the distribution of four types of magnetic field lines on the GSM equatorial plane, and Figure 4 shows some open field lines corresponding to panels (3a) and (3b). Panel (3a) shows that, at a time (2000-09-17 22:44:00 UT) of southward IMF condition as shown in Figure 2, only the southern-cusp-rooted open field lines pass through the equatorial plane, because the northern-cusp-rooted open field lines are above the equaorial plane for this time as shown in panels (4a1) and (4a2). This is the typical structure of the magnetotail for southward IMF conditions. Note that at another southward IMF time (2000-09-17 22:00:00 UT) , the open field part of panel (3a) becomes yellow (not shown) because all the southern lobe field lines are below the equatorial plane at this moment.

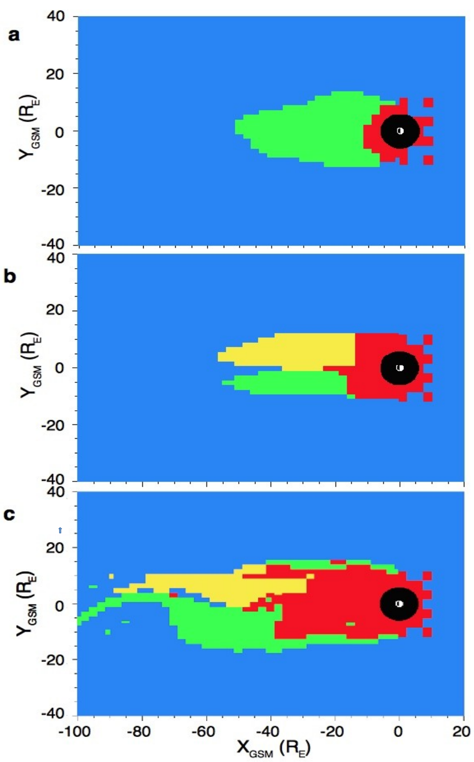

Figure 3. Distribution of four types of magnetic field lines on the GSM equatorial plane. The blue, red, green, or yellow area indicates IMF field lines, closed field lines, southern-cusp-rooted open field lines, or northern-cusp-rooted open field lines passing through it, respectively. Panels (a) and (b) are from BATS-R-US simulation, and panel (c) is from OpenGGCM simulation. The time stamp of panel (a) is 2000-09-17 22:44:00 UT, and panels (b) and (c) have the same time stamp of 2000-09-18 04:20:00 UT.

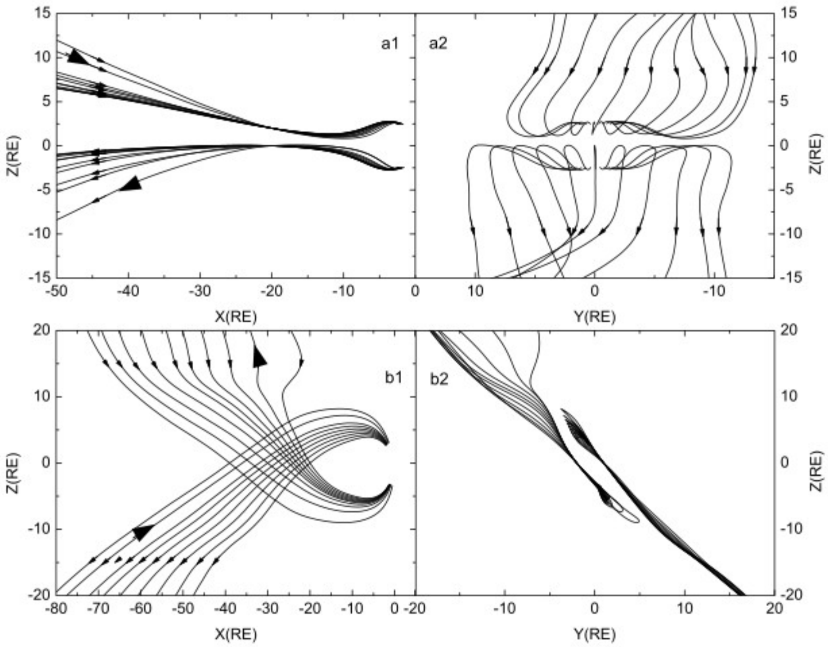

Figure 4. Open field lines under southward IMF conditions (a1, a2) and northward IMF conditions (b1, b2). Panels (a1) and (a2) are corresponding to panel (3a). Panels (b1) and (b2) are corresponding to panel (3b).

When IMF is northward, the magnetotail configuration changes dramatically. Both panel (3b) and panel (3c), which are results from different models for the same event and have the same simulation time stamp, show that there are two different domains of open field lines passing through the equatorial plane at the time of 2000-09-18 04:20:00 UT corresponding to northward IMF conditions. Some of the open field lines from these two domains are shown in panel (4b1) and panel (4b2). In contrast to the open field lines under southward IMF conditions, which stay in northern (southern) part of the tail for northern-cusp-rooted (southern-cusp-rooted) open lines, these open field lines always extend a domain from northern (southern) cusp toward the southern (northern) IMF and thus always pass through the equatorial plane.

3.2 Magnetotail under northward IMF conditions with dominant B*y*

Figure 5 shows the topology distribution of magnetic field lines when IMF is northward and has a dominant dawn-dusk component *By*. During the time from 2000-09-18 00:12:00 UT to 2000-09-18 00:30:00 UT, IMF |*By*| is much greater than IMF *Bz*, and the corresponding IMF clock angle is about 80°–90°, as shown in Figure 2. During this time period, two long open field domains form along the dawnside and duskside of the magnetotail, respectively. Here, the duskside (dawnside) domain is composed of open field lines that root in southern (northern) cusp and connect to the northern (southern) IMF. The BATS-R-US simulation results of panels (5a1) and (5a2) show that these two open domains are seperated by IMF, while the OpenGGCM simulation results of panels (5b1) and (5b2) show that these two open domains contact with each other or are very close to each other. At the same time, the BATS-R-US results show a small closed field domain, while the OpenGGCM results show a stretched and elongated closed field domain.

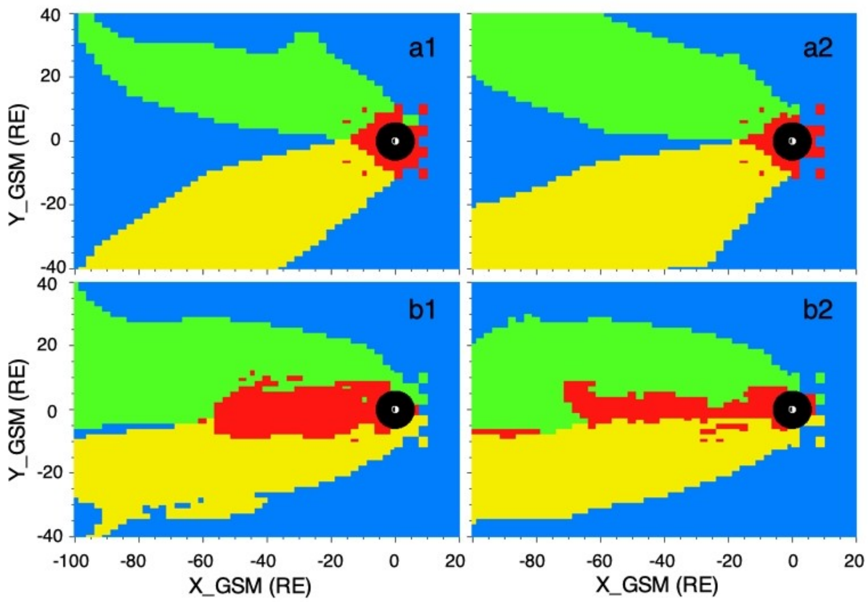

Figure 5. Topology distribution of magnetic field lines. The color means the same as Figure 3. The time stamp of (a1) and (b1) is 2000-09-18 00:12:00 UT, and the time stamp of (a2) and (b2) is 2000-09-18 00:30:00 UT. Panels (a1) and (a2) are BATS-R-US simulation results, and panels (b1) and (b2) are OpenGGCM simulation results.

3.3 Magnetotail under northward IMF conditions with less significant *By*

Figure 6 shows the topology distribution of magnetic field lines when IMF is northward and has a less significant *By*. This figure shows the minimal open status of the magnetosphere during this event. The time stamp of panels (a1) and (b1) is 2000-09-18 03:58:00 UT

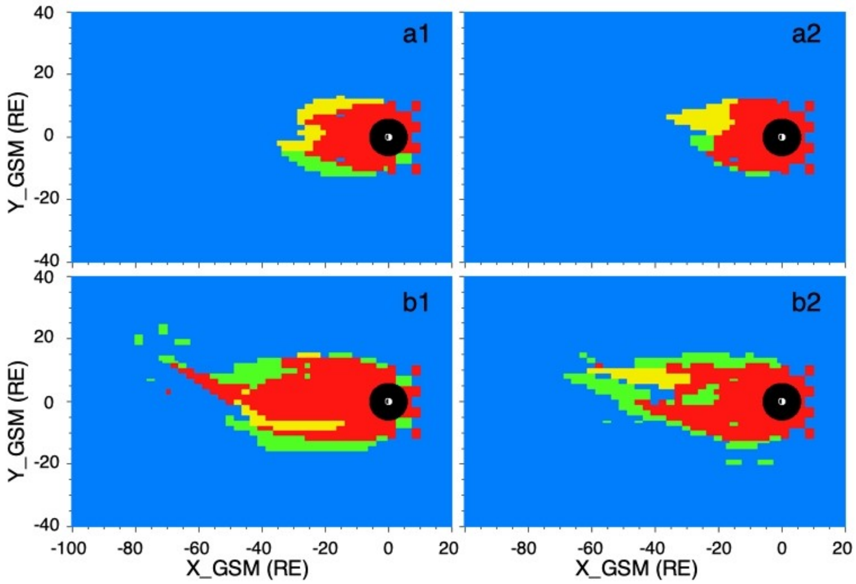

Figure 6. Topology distribution of magnetic field lines. The color means the same as Figure3. The time stamp of (a1) and (b1) is 2000-09-18 03:58:00 UT, and the time stamp of (a2) and (b2) is 2000-09-18 04:32:00 UT. Panels (a1) and (a2) are BATS-R-US simulation results, and panels (b1) and (b2) are OpenGGCM simulation results.

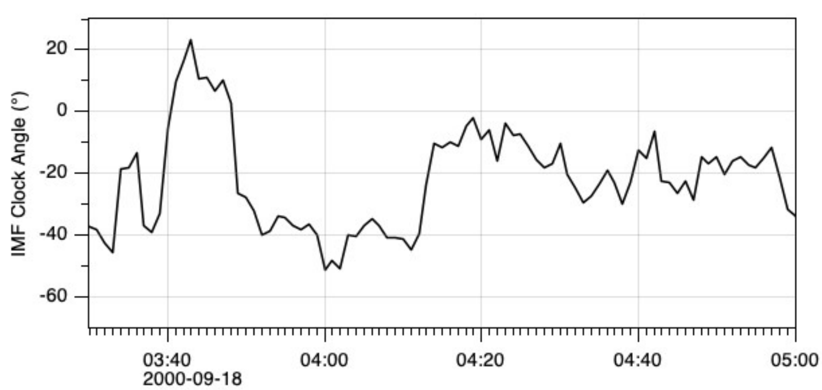

Figure 7. IMF clock angle at the nose of magnetopause from 2000-09-18 03:30:00 UT to 05:00:00 UT.

corresponding to an IMF clock angle of -36° at the nose of magnetopause. Before this time stamp and during the time period from 2000-09-18 03:44:00 UT to 2000-09-18 03:48:00 UT, IMF |*By*| is much less than IMF *Bz*, and the corresponding IMF clock angle is about 3°–10°, as shown in Figure 7. The time stamp of panels (a2) and (b2) is 2000-09-18 04:32:00 UT corresponding to an IMF clock angle of -25° at the nose of magnetopause. Before this time stamp and during the time period from 2000-09-18 04:14:00 UT to 2000-09-18 04:27:00 UT, IMF |*By*| is much less than IMF *Bz*, and the corresponding IMF clock angle is about -2°–-15°, as shown in Figure 7. Considering that there is a time delay between the arrival of an IMF field line at the nose of the magnetopause and the forming of a new open field line in the tail from this IMF field line, it seems that the magnetosphere is mostly closed when IMF clock angle is between ~-10° and ~10°.

Panels (6a1) and (6a2) resulted from BATS-R-US simulation show a nearly closed and much shrinked magnetosphere. The corresponding OpenGGCM simulation results panels (6b1) and (6b2) also show a nearly closed but significantly stretched magnetospere.

3.4 Magnetotail under northward IMF conditions with significant *By*

Figure 8 shows the topology distribution of magnetic field lines when IMF is northward and has a significant *By*. During the period from 2000-09-18 05:00:00 UT to 2000-09-18 00:80:00 UT, IMF clock angle is about -50°– -20°, as shown in Figure 2. Figure 8 shows a fairly open magnetosphere and a magnetotail with a dawnside lobe and a duskside lobe. The OpenGGCM results also show an elongated closed field as in other IMF clock angle conditions shown in Figure 5 and Figure 6.

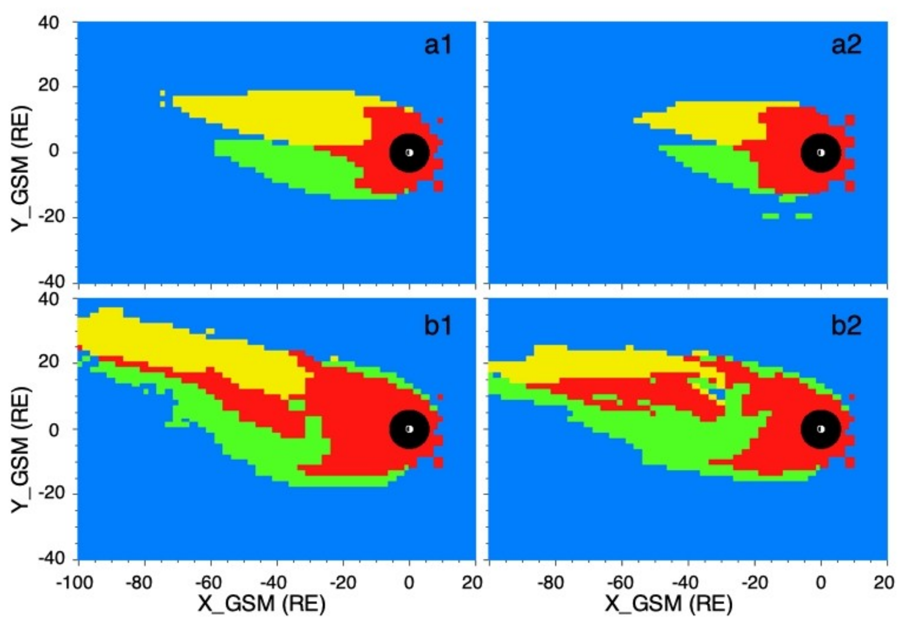

Figure 8. Topology distribution of magnetic field lines. The color means the same as Figure 3. The time stamp of (a1) and (b1) is 2000-09-18 06:00:00 UT, and the time stamp of (a2) and (b2) is 2000-09-18 07:00:00 UT. Panels (a1) and (a2) are BATS-R-US simulation results, and panels (b1) and (b2) are OpenGGCM simulation results.

3.5 Possible magnetotail reconnection under northward IMF conditions

The figures of topology distribution of magnetic field lines indicate that the two tail lobes may touch each other at a region near the X axis in the tail beyond the closed field. This contacting site may create an opportunity for reconnection since these two tail lobes are mainly opposite in magnetic direction.

The magnetic field lines shown in Figure 9 display such a reconnection process. They are computed from starting points locating near the midnight at a thin region of the contacting

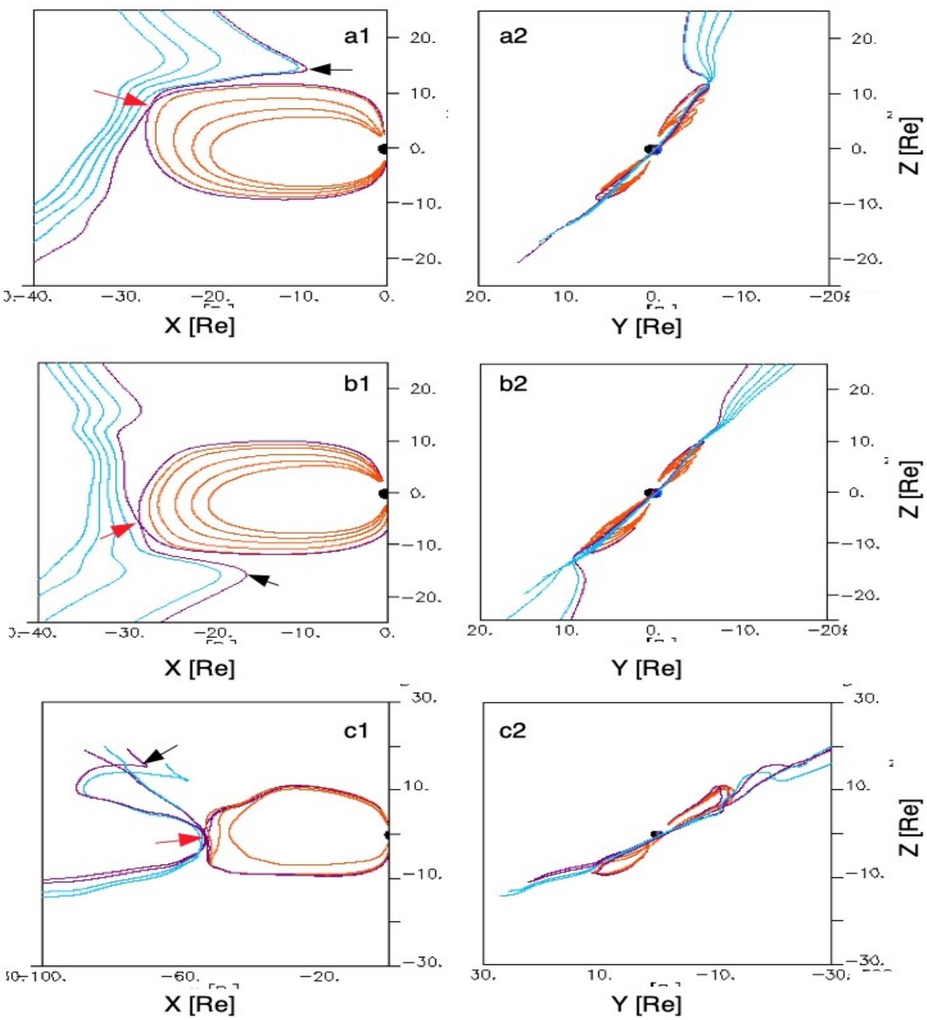

Figure 9. Magnetotail reconnection under northward IMF conditions. These field lines are computed from points at the border between the green area and yellow area in Figure 3. The blue, purple, and orange lines represent IMF, open field lines, and closed field lines, respectively. The left panels are views from GSM dawnside, and the right panels are views from the magnetotail. Panels (a1), (a2), (b1) and (b2) are results from BATS-R-US simulation, and panels (c1) and (c2) are from OpenGGCM simulation. A red arrow indicates a magnetotail reconnection site, and a black arrow indicates an open field line created by cusp reconnection.

area of these two open domains shown in panel (3b) or panel (3c), using the 3D simulation output for the time stamp of 04:20:00 UT.

In panel (9a1), a northern-cusp-rooted open field line reconnects with a southern-cusp-rooted open field line at a location above the equatorial plane and subsequently creates an IMF field line (blue) and a closed field line (orange). The location pointed by a red arrow in Figure 9 indicates a magnetotail reconnection site. Panel (9a2) shows that the field lines spread out at the reconnection site because the magnetic field at this location changes radically, resulting in these computed magnetic stream lines changing directions significantly at this turbulent site.

Panels (9b1) and (9b2) display a similar process except that it occurs at a location below the equatorial plane. Panels (9c1) and (9c2) also display a similar process but occurring at a location near the equatorial plane. One should note that the kinked sections of the field lines indicated by the black arrows in Figure 9 are results of the cusp reconnection occurring at the nightside of cusps.

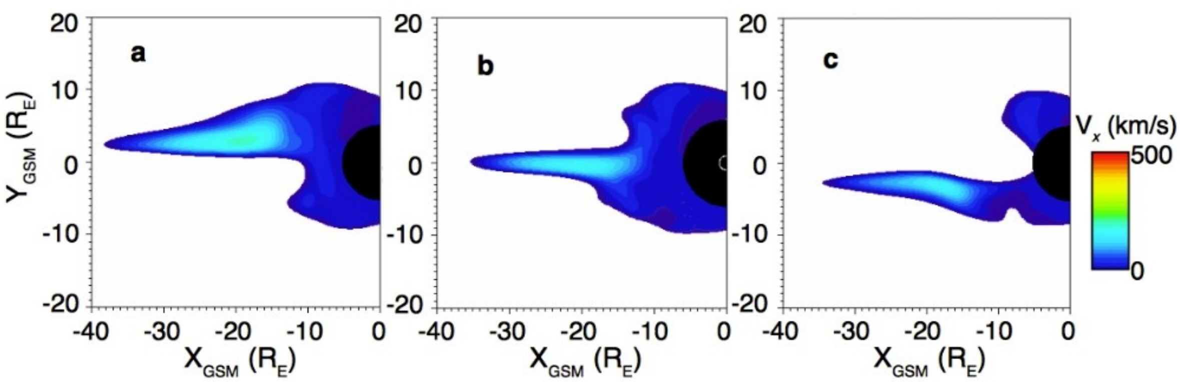

Figure 10. Distribution of plasma eathward convection velocity *Vx* on three cut planes (a) Z=-3 RE, (b) Z=0 RE, and (c) Z=3 RE. The blank area indicates tailward convection plasma.

As a result of this magnetotail reconnection process, the magnetotail should form a convection region. Figure 10 shows a distribution of the earthward convection corresponding to panels (4b1) and (4b2) for cut planes at *Z*=-3 RE (panel a), *Z*=0 RE (panel b), and *Z*=3 RE (panel c). A long and narrow significant convection zone is shown in Figure 10. All the field lines in panels (9a2), (9b2), and (9c2) show that the magnetotail is twisted for a significant angle relative to the midnight meridian plane. Therefore, the distribution of the convection region is also aligned with the twisted tail such that the southern (northern) part is at the duskside (dawnside).

4 Discussion

In this study, we show a magnetotail configuration that looks significantly different from the one developed under southward IMF conditions. It is interesting to discuss how this configuration forms and what magnetospheric or ionospheric effects it may cause.

4.1 Cusp reconnection

Obviously the magnetotail configuration is mainly affected by magnetic reconnection occuring in the magnetosphere. To understand the magnetotail configuration, we need to understand the reconnection process that occurs under northward IMF conditions.

The most well known reconnction process for northward IMF is the cusp reconnection or high-latitude reconnction first proposed by Dungey (1963) who suggested that a northward IMF would be antiparallel to the Earth's field at points poleward of the cusps and makes reconnection possible there, as shown in Figure 1. The IMF field lines may interconnect with open tail lobe field lines (Russell, 1972), or with closed geomagnetic field lines (Cowley, 1981, 1983).

Observations have provided evidences for cusp reconnection (e.g., Fuselier et al., 2000; Gosling et al., 1991; Kessel et al., 1996; Le et al., 2001; Lavraud et al., 2002; Lavraud et al., 2005a; Onsager et al., 2001; Phan et al., 2003), and global MHD models have reproduced this process (Fedder & Lyon, 1995; Gombosi et al., 1998; Guzdar et al., 2001; Ogino et al., 1994; Raeder et al., 1997).

Observations show that cusp reconnction may occur at a broad local time range of locations (Onsager et al., 2001) and can occur for IMF clock angles between -90° and 90° (Twitty et al., 2004). When geomagnetic dipole tilts sunward (antisunward), an IMF field line may first interconnect with a geomagnetic field line at northern (southern) cusp, and then at southern (northern) cusp (Lavraud et al., 2005b).

Onsager et al. (2001) reported that cusp reconnection may create new closed field lines and new open field lines with footprints in either northern or southern cusp. They also identified high-latitude closed field lines participating in cusp reconnection.

As shown in Figure 4, an open field line created by cusp reconnection always connects northern (or southern) cusp to southern (or northern) IMF and passes through the equatorial plane, in contrast to an open field line created by dayside magnetopause reconnection which always connects northern (or southern) cusp to northern (or southern) IMF.

4.2 Magnetotail formation under northward IMF conditions

This study suggests that the magnetotail configuration is mainly affected by the IMF clock angle at the nose of the magnetopause when IMF is northward. When IMF is nearly due northward, the magnetosphere is nearly closed, and the magnetotail is minimal or disappears. When IMF is northward and has a significant dawn-dusk component By, the magnetosphere is fairly open and the magnetotail usually forms into a dawnside tail lobe and a duskside tail lobe, instead of a northern tail lobe and a southern tail lobe under southward IMF conditions. When IMF is northward and has a dominant By, the magnetotail is much large and very long with a width of more than 60 RE and a length of more than 100 RE.

Since the magnetotail is mainly a topological structure, the geometric and topological property of the geomagnetic field and the IMF thus plays a dominant role in determining how cusp reconnection process occurs and consequently forms the magnetotail.

In an ideal condition in which the IMF is pure northward in GSM coordinates and the Earth's dipole tilt angle is zero, an IMF field line most likely merges with geomagnetic field at both cusps simutaniously as shown in Figure 1. This process then forms a closed field line draping the dayside magnetopause and then integrating itself into the closed field. In the night side, this process creates one new IMF field line if the reconnecting geomagnetic field line is a closed field line connecting both reconnection sites, or creates two new IMF field lines if the reconnecting geomagnetic field lines at both reconnecting sites are two open field lines, eroding the previously existing open field lines. After a period of pure northward IMF conditions, the magnetosphere may become completely closed.

However, when the IMF at the nose of the magnetopause has a significant *By* (or clock angle), the symetric field line distribution as shown in Figure 1 does not likely exist. Assuming that the IMF turns a clcok angle of 60°, the whole draped IMF field line does not likely also turn ~60° such that this IMF field line reconnections with the same closed field line at both cusps, because an IMF field line always dapes around the magnetopause anti-sunward and aligns with the solar wind velocity direction instead of the IMF clock angle. Therefore, with a significant clock angle, the probability for an IMF field line draping on northern (southern) cusp also drapes on southern (northern) cusp on the same local time location is reduced. The bigger the clock angle magnitude, the less probability of reconnecting with the same closed field line or reconnecting with geomagnetic field at both cusps simultaniously, thus the more probability of creating open field lines. Such open field lines are then convected anti-sunward and form a tail as shown by panels (4b1) and (4b2) in Figure 4. A bigger IMF clock angle magnitude thus leads to a larger and longer magnetotail.

When the northward IMF has a significant *Bx*, or the Earth's dipole has a significant tilt angle, an IMF field line may not merge with geomagnetic field simutaniously at both cusps. In this case, an open field line drapping the dayside magnetopause is probably created and convected to the night side before it can reconnect with another geomangetic field line at the other cusp.

Therefore, the magnetosphere is open most of the time even under northward IMF conditions because cusp reconnection most likely creates open field lines except for an ideal pure northward IMF condition which rarely accurs. The open field lines all pass through the equatorial plane because they always connect northern (southern) cusp with southern (northern) IMF. The open field lines created by cusp reconnection usually form a tail lobe in the dawnside and another tail lobe in the duskside since the IMF field lines draping at northern magnetopause most likely are convected to one side of the magnetotail, and the IMF field lines draping at southern magnetopause most likely are convected to the other side. Figure 5 and Figure 8 indicate that the southern-cusp-rooted tail lobe is in the duskside (dawnside) for positive (negative) IMF *By* and the northern-cusp-rooted tail lobe is in the other side.

Besides IMF clock angle and dipole tilt angle, other IMF and solar wind parameters may have some degree of effects on the formation of magnetotail. Figure 8 shows that the dawnside lobe seems to be pushed toward duskside. It may relate to solar wind velocity *Vy* component since *Vy* is on 100 km/s level from 2000-09-18 04:00:00 UT to 2000-09-18 08:00:00 UT, but is mainly less than 50 km/s before this period. Sometimes the topological distribution map shows only one type of open field lines. It is possible a result of a significant IMF *Bx* component or a significant dipole tilt angle that causes reconnection to only occur at one cusp. We havn't found any significant relation between the tail configuration and solar wind density or temperature. The effect of IMF magnitude, solar wind *Vz*, or *Vx* needs more study.

In this study, we also simulate another event from 2000:08:12 20:00 UT to 2000:08:13 02:00 UT during which the IMF clock angle gradually changes from ~90° to ~10°. The simulation results show that the magnetotail gradually changes from one like Figure 5 to the one like Figure 8.

The field lines shown in Figure 4 and Figure 9 suggest that a neutral sheet with a significant angle relative to the equatorial plane may form in the tail. Observations show that neutral sheet twists a larger angle for northward IMF than for southward IMF when IMF *By* is significant (Case et al., 2018; Maezawa & Hori, 1998; Xiao et al., 2016). Analysing data from Cluster, Geotail, and Interball, Petrukovich et. al. (2003) found that the plasma sheet twists a very large angle under northward IMF conditions with a significant *By*.

4.3 Magnetotail reconnection and substorms under northward IMF conditions

From WIND data, Oieroset et. al. (2000, 2004) reported five fast flow events occuring in the tail about 25–60 RE during a fourd-day period with mainly northward IMF conditions. The analyses of these fast flows suggest that quasi-steady reconnection can occur in the mid-magnetotail region during periods of persistent northward IMF.

It is usually believed that substorm is not likely to occur under long period of northward IMF conditions. However, some substorm events occurring during long period of northward IMF conditions have been reported.

After studying more than 50 auroral substorms, Akasofu et al. (1973) found that, during quiet periods, auroral substorms are quite common along the contracted oval even when the IMF *Bz* is positive. Petrukovich et al. (2000) investegated 43 small substorms and found that typical IMF direction during substorm growth phases was azimuthal (with dominating *By* and small positive or negative *Bz*), and that no small substorms associated with definitely northward IMF ($Bz > |By|$).

Lee et al. (2010) reported several substorms observed under northward IMF conditions. The two event periods in this study are also the events reported by Lee et al. (2010). They report substorm onsets at 2000-08-13 00:00:05 UT, 2000-09-18 04:10:00 UT, 2000-09-18 06:20:00 UT, and 2000-09-18 10:07:00 UT. These time stamps are at a time that northward IMF conditions with significant clock angle has lasted for at least 4 hours.

Miyashita et al. (2011) reported 11 very weak to moderate substorm expansions occurred during a period of more than 20 hours of northward IMF conditions on 19 January 1998. They suggested that the large IMF $|By|$ is a very important factor.

A statistical study performed by Peng et al. (2013) suggests that duration of northward IMF, IMF *By* component, dynamic pressure, storms, and pre-southward IMF conditions are related to the occurrence of substorm under northward IMF conditions. Zhang et al. (2015) reported X lines in the tail for northward IMF with AE index in a range of 50–70 nT. Du et al. (2008) reported an anomalous geomagnetic storm whose main phase occurred during Northward IMF conditions.

If the northward IMF with significant *By* persists for a substantial time period, the tail lobes and thus the magnetic energy in the tail will eventually grow to a degree to trigger a reconnection process as shown in Figure 9 or even a substorm to release the energy.

The field lines shown in Figure 4 and Figure 9 suggest that the magnetic pressure that pushes open field lines toward the reconnection center, where magnetic pressure is low, mainly from dawnside and duskside of the tail. It thus does not have much pressure on the newly closed field lines from the north and the south. Therefore, the pre-reconnection field lines and the newly closed fields are not stretched significantly and can only result in a weak convection region. In contrast, the pre-reconnection field lines and the newly created closed field lines formed during a magnetotail reconnection under southward IMF conditions are usually greatly stretched. Therefore, magnetotail convection and substorm, if any, are usually weak under northward IMF conditions.

Our simulation results suggest that the magnetotail configuration is rather sensitive to IMF clock angle, IMF *Bx*, or geomagnetic dipole tilt angle. Since IMF rarely has a stable clock angle, it is not often for such dawn-dusk tail lobe reconnection to occur for a substantial time. The low probability of occurrence and the resulting weak convection explain why it is not often to observe magnetotail reconnection or substorm under northward IMF conditions.

To explain the Geotail observations of magnetotail convection for periods of quiet time and northward IMF with $|By| \geq Bz$, Nishida et al. (1998) proposed a model (see Figure 9 in their paper) that is similar to the magnetotail configuration presented here. Here, we present a more realistic view of this model using simulation data.

This magnetotail configuration and the related reconnection process also provide a way for solar wind plasma entry into the plasma sheet in the mid-tail region since the newly closed field lines catch the solar wind plasma on the reconnecting open field lines.

4.4 Ionosphere observations related to northward IMF with significant *By*

Although this study doesn’t inspect ionosphere effects from simulation results, we would like to point out some ionosphere observations under northward IMF conditions with significant *By* since the magnetotail configuration presented here may provide an alternative perspective for the observed phenomenon.

Using the Dynamics Explorer (DE) 2 data, Taguchi et al. (1992) examined *By*−controlled convection and field−aligned currents in the midnight sector for northward IMF. Their findings are quoted as following. “When IMF is stable and when its magnitude is large, a coherent *By*−controlled convection exists near the midnight auroral oval in the ionosphere having adequate conductivities. When *By* is negative, the convection consists of a westward (eastward) plasma flow at the lower latitudes and an eastward (westward) plasma flow at the higher latitudes in the midnight sector in the northern (southern) ionosphere. When *By* is positive, the flow directions are reversed.” (Taguchi et al., 1992).

Grocott et al. (2005) presented interhemispheric radar observations interpreted as the ionospheric response to tail reconnection during northward IMF intervals. SuperDARN observations for days on 21–22 February and 26–27 April 2000 showed bursts of flow in the midnight sector for both hemispheres of ionosphere during northward IMF with a significant *By*. The bursts were westwards (eastwards) in the Northern (Southern) Hemisphere during the negative *By* interval. Their directions were reversed during the positive *By* interval.

These ionosphere phenomena seem to relate to the formation of dawn-dusk tail lobes and the resulted reconnection process when IMF is northward with a significant *By*. For example, the twisted newly created closed field lines shown in Figure 9 most likely create the dawn-dusk ionospheric convection when they adjust themselves into normal closed field lines.

4.4 BATS-R-US vs OpenGGCM

For this study, we use two different global magnetosphere models through NASA CCMC portal. One is the BATS-R-US which has been chosen by NOAA Space Weather Prediction Center to be part of the operational space weather model. The other is the OpenGGCM which has been used in simulating some events with well agreement with observations, especially for events under northward IMF conditions (Raeder et al., 1995; Li et al., 2005; Li et al., 2009; Li et al., 2017). In this study, both models simulate the same events but have significant differences in results due to their differences in implementing methods and different coupled ionosphere models (Raeder, 2000). For example, BATS-R-US seems to have smaller closed field and more regular shape of the magnetosphere, while OpenGGCM has longer closed field and longer magnetotail with a more irregular form.

However the differences are, they have two basic common results. One is that a domain of open field lines connecting northern cusp to southern IMF will form in one side (dawn or dusk) of the magnetotail while another domain of open field lines connecting southern cusp to northern IMF will form in the other side of the magnetotail under northward IMF conditions with significant *By*. This result is determined by the geometry and topology properties of the Earth's dipole field and the IMF in front of the magnetopause. The other common result is that these two open domains may contact each other at some point and trigger a reconnection process.

5 Conclusions

On the one hand, when the IMF at the magnetopause is southward, the reconnection process at dayside magnetopause creates a northern open field tail lobe and a southern open field tail lobe with opposite magnetic field direction. On the other hand, when the IMF is northward with a significant dawn-dusk component *By*, cusp reconnection is possible to create a dawnside open field tail lobe and a duskside open field tail lobe with opposite magnetic field direction. Such a tail lobe are open field lines root in northern (southern) cusp and connect with southern (northern) IMF. The bigger the magnitude of IMF clock angle, the longer and wider magnetotail. A magnetic reconnection process may occur in the magnetotail when the dawnside and duskside tail lobes contact with each other. A substorm is also possible to occur due to such reconnection process.

Acknowledgments

This work was carried out using the OpenGGCM tools developed at the University of New Hampshire and the SWMF/BATS-R-US tools developed at the University of Michigan's Center for Space Environment Modeling (CSEM). Simulation results and analysis tools have been provided by the NASA Community Coordinated Modeling Center (CCMC) at Goddard Space Flight Center through their public Runs on Request system (http://ccmc.gsfc.nasa.gov). All the simulation data can be accessed through CCMC website (https://ccmc.gsfc.nasa.gov/results/). The solar wind and IMF data are from NASA CDAWeb

OMNI datasets (https://cdaweb.gsfc.nasa.gov/). This work was supported by College of Science at the Zhejiang University of Technology.

References

Akasofu, S.‐I., Perreault, P. D., Yasuhara, F., & Meng, C.‐I. (1973). Auroral substorms and the interplanetary magnetic field. *Journal of Geophysical Research: Space Physics*, 78(31), 7490–7508. https://doi.org/10.1029/JA078i031p07490

Case, N. A., Grocott, A., Martin, C. J., Haaland, S., & Nagai, T. (2018). Response of Earth's neutral sheet to reversals in the IMF *By* component. *Journal of Geophysical Research: Space Physics*, 123, 8206–8218. https://doi.org/10.1029/2018JA025712

Cowley, S. W. H. (1981). Magnetospheric and ionospheric flow and the interplanetary magnetic field. In *The Physical Basis of the Ionosphere in the Solar-Terrestrial System*, AGARD Conference Proceeding, 295, 4/1–4/14.

Cowley, S. W. H. (1983). Interpretation of observed relations between solar wind characteristics and effects at ionospheric altitudes. In B. Hultquist and T. Hagfors (Eds.), *High Latitude Space Plasma Physics* (pp. 225). Plenum, New York

Du, A. M., Tsurutani, B. T. & Sun, W. (2008). Anomalous geomagnetic storm of 21-22 January 2005: A storm main phase during northward IMFs. *Journal of Geophysical Research: Space Physics*, 113, A10214. https://doi.org/10.1029/2008JA013284

Dungey, J. W. (1961). Interplanetary magnetic field and the auroral zones. *Physical Review Letters,* 6, 47-48.

Dungey, J. W. (1963). The structure of the exosphere or adventures in velocity space. In C. DeWitt, J. Hieblot, & A. Lebeau (Eds.), *Geophysics, The Earth's Environment*, (pp. 503-550). New York, NY: Gordon and Breach.

Fedder, J. A., & Lyon, J. G. (1995). The Earth's magnetosphere is 165 RE long: Self-consistent currents, convection, magnetospheric structure, and processes for northward interplanetary magnetic field. *Journal of Geophysical Research: Space Physics*, 100, 3623.

Fuller-Rowell, T. J., Rees, D., Quegan, S., Moffett, R. J., Codrescu, M. V., & Millward, G. H. (1996). A coupled thermosphere-ionosphere model (CTIM). In R. W. Schunk, *STEP Report*, (pp. 217). Boulder, CO: NOAA.

Fuselier, S. A., Trattner, K. J., & Petrinec, S. M. (2000). Cusp observations of high- and low-latitude reconnection for northward interplanetary field. *Journal of Geophysical Research: Space Physics*, 105, 253-256.

Gombosi, T. I., DeZeeuw, D. L., Groth, C. P. T., Powell, K. G. & Song, P., (1998). The length of the magnetotail for northward IMF: Results of 3D MHD simulations. *Physics of Space Plasmas*, 15, 121.

Gosling, J. T., Thomsen, M. F., Bame, S. J., & Elphic, R. C. (1991). Observations of reconnection of interplanetary and lobe magnetic field lines at the high-latitude magnetopause. *Journal of Geophysical Research: Space Physics*, 96, 14,097.

Grocott, A., Yeoman, T. K., Milan, S. E., & Cowley, S. W. H. (2005). Interhemispheric observations of the ionospheric signature of tail reconnection during IMF-northward nonsubstorm intervals. *Annales Geophysicae*, 23, 1763–1770. https://doi.org/10.5194/angeo-23-1763-2005

Guzdar, P. N., Shao, X., Goodrich, C. C., Papadopoulos, K., Wiltberger, M. J., & Lyon, J. G. (2001). Three-dimensional MHD simulations of the steady state magnetosphere with northward interplanetary magnetic field. *Journal of Geophysical Research: Space Physics*, 106, 275.

Kessel, R. L., Chen, S.-H., Green, J. L., Fung, S. F., Boardsen, S. A., Tan, L. C., et al. (1996). Evidence of high-latitude reconnection during northward IMF: Hawkeye observations. *Geophysical Research Letters*, 23, 583.

Lavraud, B., Dunlop, M. W., Phan, T. D., Rème, H., Bosqued, J.-M., Dandouras, I., et al. (2002). et al., Cluster observations of the exterior cusp and its surrounding boundaries under northward IMF. *Geophysical Research Letters*, 29(20), 1995. https://doi.org/10.1029/2002GL015464

Lavraud, B., Fedorov, A., Budnik, E., Thomsen, M. F., Grigoriev, A., Cargill, P. J., et al. (2005a), High-altitude cusp flow dependence on IMF orientation: A 3-year Cluster statistical study. *Journal of Geophysical Research: Space Physics*, 110, A02209. https://doi.org/10.1029/2004JA010804

Lavraud, B., Thomsen, M. F., Taylor, M. G. G. T., Wang, Y. L., Phan, T. D., Schwartz, S. J., et al. (2005b). Characteristics of the magnetosheath electron boundary layer under northward interplanetary magnetic field: Implications for high-latitude reconnection. *Journal of Geophysical Research: Space Physics*, 110, A06209. https://doi.org/10.1029/2004JA010808

Lavraud, B., Thomsen, M. F., Lefebvre, B., Schwartz, S. J., Seki, K., Phan, T. D., et al. (2006). Evidence for newly closed magnetosheath field lines at the dayside magnetopause under northward IMF. *Journal of Geophysical Research: Space Physics*, 111, A05211. https://doi.org/10.1029/2005JA011266

Le, G., Raeder, J., Russell, C. T., Lu, G., Petrinec, S. M., & Mozer, F. S. (2001). Polar cusp and vicinity under strongly northward IMF on April 11, 1997: Observations and MHD simulations. *Journal of Geophysical Research: Space Physics*, 106, 21,083.

Lee, D.-Y., Choi, K.-C., Ohtani, S., Lee, J. H., Kim, K. C., Park, K. S., & Kim, K.-H. (2010). Can intense substorms occur under northward IMF conditions? *Journal of Geophysical Research: Space Physics,* 115, A01211. https://doi.org/10.1029/2009JA014480

Li, W., Raeder, J., Dorelli, J., Øieroset, M., & Phan, T. D. (2005). Plasma sheet formation during long period of northward IMF. *Geophysical Research Letters*, 32, L12S08. https://doi.org/10.1029/2004GL021524

Li, W., Raeder, J., Thomsen, M. F., & Lavraud, B. (2008). Solar wind plasma entry into the magnetosphere under northward IMF conditions. *Journal of Geophysical Research: Space Physics,* 113, A04204. https://doi.org/10.1029/2007JA012604

Li, W., Raeder, J., Øieroset, M., & Phan, T. D. (2009). Cold dense magnetopause boundary layer under northward IMF: Results from THEMIS and MHD simulations. *Journal of Geophysical Research: Space Physics,* 114, A00C15. https://doi.org/10.1029/2008JA013497

Li, W.−H., Raeder, J., Thomsen, M. F., Lavraud, B., Lü, L.−Z., & Liang, E.−W. (2017). The formation of superdense plasma sheet in association with the IMF turning from northward to southward. *Journal of Geophysical Research: Space Physics*, 122, 2936–2955, https://doi.org/10.1002/2016JA023373

Maezawa, K., & Hori, T. (1998). The Distant Magnetotail: Its Structure, IMF Dependence, and Thermal Properties. In *New Perspectives on the Earth's Magnetotail* (pp. 1-19). Washington, DC: American Geophysical Union. https://doi.org/10.1029/GM105p0001

Miyashita, Y., Kamide, Y., Liou, K., Wu, C.−C., Ieda, A., Nishitani, N., et al. (2011). Successive substorm expansions during a period of prolonged northward interplanetary magnetic field. *Journal of Geophysical Research: Space Physics*, 116, A09221. https://doi.org/10.1029/2011JA016719

Nishida, A., Mukai, T., Yamamoto, T., Kokubun, S., & Maezawa, K. (1998). A unified model of the magnetotail convection in geomagnetically quiet and active times. *Journal of Geophysical Research: Space Physics*, 103, 4409-4418. https://doi.org/10.1029/97JA01617

Ogino, T., Walker, R. J., & Ashour-Abdalla, M. (1994). A global magnetohydrodynamic simulation of the response of of the magnetosphere to a northward turning of the interplanetary magnetic field. *Journal of Geophysical Research: Space Physics*, 99, 11,027.

Øieroset, M., Phan, T. D., Lin, R. P., & Sonnerup, B. U. O. (2000). Walén and variance analyses of high-speed flows observed by Wind in the midtail plasma sheet: Evidence for reconnection. *Journal of Geophysical Research: Space Physics*, 105, 25,247.

Øieroset, M., Phan, T. D., Fujimoto, M., & Lin, R. P. (2004). Distant magnetotail reconnection and the coupling to the near-Earth plasma sheet: Wind and Geotail case study. *Geophysical Research Letters*, 31, L18805. https://doi.org/10.1029/2004GL020321

Øieroset, M., Phan, T. D., Fairfield, D. H., Raeder, J., Gosling, J. T., Drake, J. F., & Lin, R. P. (2008). The existence and properties of the distant magnetotail during 32 hours of strongly northward interplanetary magnetic field. *Journal of Geophysical Research: Space Physics,* 113, A04206. https://doi.org/10.1029/2007JA012679

Onsager, T. G., Scudder, J. D., Lockwood, M., & Russell, C. T. (2001). Reconnection at the high-latitude magnetopause during northward interplanetary magnetic field conditions. *Journal of Geophysical Research: Space Physics,* 106, 25467-25488. https://doi.org/10.1029/2000JA000444

Park, K. S., Lee, D.−Y., Ogino, T., & Lee, D. H. (2015). MHD simulations using average solar wind conditions for substorms observed under northward IMF conditions. *Journal of Geophysical Research: Space Physics,* 120, 7672–7686. https://doi.org/10.1002/2015JA021005

Petrukovich, A. A., Baumjohann, W., Nakamura, R., Mukai, T., & Troshichev, O. A. (2000). Small substorms: Solar wind input and magnetotail dynamics. *Journal of Geophysical Research: Space Physics*, 105, 21, 109. https://doi.org/10.1029/ 2000JA900057

Petrukovich, A. A., Baumjohann, W., Nakamura, R., Balogh, A., Mukai, T., Glassmeier, K.-H., et al. (2003). Plasma sheet structure during strongly northward IMF. *Journal of Geophysical Research: Space Physics*, 108(A6), 1258. https://doi.org/10.1029/2002JA009738

Peng, Z., Wang, C., Yang, Y. F., Li, H., Hu, Y. Q., & Du, J. (2013). Substorms under northward interplanetary magnetic field: Statistical study. *Journal of Geophysical Research: Space Physics,* 118, 364–374. https://doi.org/10.1029/2012JA018065

Phan, T. D. Frey, H. U., Frey, S., Peticolas, L., Fuselier, S., Carlson, C., et al. (2003). Simultaneous Cluster and IMAGE observations of cusp reconnection and auroral proton spot for northward IMF. *Geophysical Research Letters,* 30, 1509-1512. https://doi.org/10.1029/2003GL016885

Powell, K.G., Roe, P.L., Linde, T.J., Gombosi, T.I., & De Zeeuw, D.L. (1999). A solution-adaptive upwind scheme for ideal magnetohydrodynamics. *Journal of Computational Physics*, 154, 284-309. https://doi.org/10.1006/jcph.1999.6299

Raeder, J., Walker, R. J. & Ashour-Abdalla M. (1995). The structure of the distant geomagnetic tail during long periods of northward IMF. *Geophysical Research Letters*, 22, 349-352. https://doi.org/10.1029/94GL03380

Raeder, J., Berchem, J., Ashour-Abdalla, M., Frank, L. A., Paterson, W. R., Ackerson, K. L., et al. (1997). Boundary layer formation in the magnetotail: Geotail observations and comparisons with a global MHD model. *Geophysical Research Letters*, 24, 951.

Raeder, J. (2000). Reply to “Comment on ‘Modeling the magnetosphere for northward interplanetary magnetic field: Effects of electrical resistivity’ by Joachim Raeder”. *Journal of Geophysical Research: Space Physics*, 105, 13149–13153. https://doi.org/10.1029/2000JA000006

Raeder, J. (2003), Global geospace modeling: Tutorial and review. In J. Büchner, C. T. Dum, & M. Scholer (Eds.), *Space Plasma Simulation.* New York, NY: Springer.

Rosenqvist, L., Kullen, A., & Buchert, S.(2007). An unusual giant spiral arc in the polar cap region during the northward phase of a Coronal Mass Ejection. *Annales Geophysicae*, 25, 507–517. https://doi.org/10.5194/angeo-25-507-2007

Russell, C. T. (1972). The configuration of the magnetosphere. In E. R. Dyer, *Critical Problems of Magnetospheric Physics* (pp. 1). Washington, DC: National Academic of Science.

Song, P., DeZeeuw, D. L., Gombosi, T. I., Groth, C. P. T., & Powell, K. G. (1999). A numerical study of solar wind-magnetosphere interaction for northward interplanetary magnetic field. *Journal of Geophysical Research: Space Physics,* 104, 28361–28378. https://doi.org/10.1029/1999JA900378

Taguchi, S. (1992). *By*−controlled field−aligned currents near midnight auroral oval during northward interplanetary magnetic field. *Journal of Geophysical Research: Space Physics*, 97(A8), 12231–12243. https://doi.org/10.1029/92JA00548

Tóth, G., van der Holst, B., Sokolov, I.V., De Zeeuw, D.L., Gombosi, T.I., Fang, F., et al. (2012). Adaptive numerical algorithms in space weather modeling. *Journal of Computational Physics*, 231, 870-903. https://doi.org/10.1016/j.jcp.2011.02.006

Twitty, C., Phan, T. D., Paschmann, G., Lavraud, B., H. Rème, H., & Dunlop, M. (2004). Cluster survey of cusp reconnection and its IMF dependence. *Geophysical Research Letters*, 31, L19808. https://doi.org/10.1029/2004GL020646

Xiao, S., Zhang, T., Ge, Y., Wang, G., Baumjohann, W., & Nakamura, R. (2016). A statistical study on the shape and position of the magnetotail neutral sheet. *Annales Geophysicae*, 34, 303-311. https://doi.org/10.5194/angeo-34-303-2016

Zhang, L. Q., Wang, J. Y., Baumjohann, W., Rème, H., Dai, L., Dunlop, M. W., et al. (2015). X lines in the magnetotail for southward and northward IMF conditions. *Journal of Geophysical Research: Space Physics,* 120, 7764-7773. https://doi.org/10.1002/2015JA021503